Digital Control Law Synthesis in the w' Domain

R.F. Whitbeck* and L.G. Hofmann†
Systems Technology, Inc., Hawthorne, Calif.

Utility of w' transform domain analysis/synthesis procedures for linear, constant, single-rate sampled-data systems is explored. Basic properties of the w' domain are reviewed and compared with corresponding z-,w-, and s-domain properties. The main contribution of the paper is recognition that sampling and data-hold operations are modeled exactly in the w' domain, regardless of the sampling rate employed, and that the w' variable is analogous to the s variable in the sense that all familiar frequency domain design concepts, procedures, and interpretations can be carried over directly. Moreover, the imaginary part of w' approximates angular frequency ω for $|\omega| < \pi/2T$, which further facilitates interpretation. Two example applications illustrate the procedure and make clear (by means of transfer functions and Bode plots) the nonminimum phase effects of sampling and data-hold operations and of sampling rate. It is demonstrated that acceptable closed-loop performance can be achieved at sampling rates that are an order of magnitude less than those employed when an emulation design approach is used.

Nomenclature

$H(\cdot)$ = transfer function in domain indicated in $(\cdot)$
n_z = incremental load factor measured 7 ft forward of c.g., g
$N^{(\cdot)}_{[\cdot]}$ = numerator polynomial of transfer function, response of $(\cdot)$ to input $[\cdot]$
$N^{(\cdot)[\cdot]}_{[\cdot]\langle\cdot\rangle}$ = coupling numerator polynomial, $N^{(\cdot)[\cdot]}_{[\cdot]\langle\cdot\rangle} = [N^{(\cdot)}_{[\cdot]} N^{[\cdot]}_{\langle\cdot\rangle} - N^{(\cdot)}_{\langle\cdot\rangle} N^{[\cdot]}_{[\cdot]}]/\Delta$
q = pitch rate, rad/s
q_g = pitch rate measured 7 ft aft of c.g., rad/s
R = command input to pitch stability and command augmentation system, rad/s
s = Laplace transform variable, a complex number
T = sampling period
v = imaginary part of w (dimensionless)
w = w-transform variable, a complex number related to z by $w = (z-1)/(z+1)$
w' = w'-transform variable, a complex number related to z by $w' = (2/T)(z-1)/(z+1)$
x = state variable
x_b = displacement in normalized first longitudinal fuselage bending mode coordinate, ft
z = z-transform variable, a complex number
α = inertial component of angle of attack, rad
α_g = disturbance component of aerodynamic angle of attack, rad
δ_e = elevator control input, rad
Δ = characteristic polynomial of transfer function
ν = imaginary part of w', s^{-1}
ω = angular frequency, imaginary part of s, rad/s
$[\cdot]^T$ = $[\cdot]$ sampled with sampling period T

Introduction

DURING the 1950's and 1960's, the need for simulating open- and closed-loop aircraft responses furnished an appreciable impetus for the development and refinement of discrete algorithms for the simulation of continuous systems using digital computers.[1-3] Thus, the Tustin transform method and other similar techniques for the approximate discretization of continuous systems made it feasible to replace analog computers with digital computers for the simulation phases of a design effort. Even now, this approach commonly is applied to design digital control laws for fly-by-wire aircraft. First a continuous control law is synthesized, and then it is adapted for digital implementation using one of the approximate discretization methods originally developed for simulation.[4-6] This procedure is called emulation.

This application of emulation for the design of a digital controller is motivated both by a fundamental reliance on system design criteria developed for analog systems and the justifiable desire to preserve the large body of design experience built up over the past 25 years. Emulation is an approximate procedure when the Tustin transform or other "direct substitution" methods are used. In general, emulation procedures fail to account for multiplexer/data bus effects and, more importantly, require use of high update rates (short computation frame times) in order for the inherent approximations to be valid. Thus there is a need for a direct digital design procedure that is exact (in distinction to approximate), accounts for the effects of data holds, computational delays, etc., and yet preserves the experience and physical insight developed over the years using conventional design procedures. The purpose of this paper is to highlight the properties of a design domain wherein these objectives are realized.

Specifically, attention is focused on the w' domain: a domain related to the well-known w domain[7] by an all-important scale factor. It is a domain wherein the nonminimum phase effects of the sampling and data-hold operations can be accounted for directly using conventional frequency domain design tools such as root locus and Bode plots. These conventional frequency domain design tools can be used to considerably greater advantage in the w' domain than in the w or z domains because several more powerful analogies between the s domain and the w' domain exist. These analogies are, in a sense, the key to exploiting the w' domain for design purposes, making direct design in the w' domain an attractive alternative to design by emulation.

The w' technique is, like many other analysis techniques, an aid to understanding the problem. As such, it will be more valuable to some individuals than to others. Value usually will be perceived as greater by individuals customarily using classical (frequency, z or w domain) design or emulation design techniques, and by those having significant experience with computer-aided problem solution using these classical techniques. The natural tendency is for an individual to continue using those methods and techniques he is most familiar and comfortable with.

Received Oct. 28, 1977; revision received March 3, 1978.

Index categories: Analytical and Numerical Methods; Guidance and Control; LV/M Dynamics and Control.

*Principal Research Engineer.
†Principal Research Engineer. Member AIAA.

In the sections that follow, we first review basic properties that make the w' domain preferable to the z or w domain. Following this, illustrative examples are used to highlight the analogies between s and w'. Next we demonstrate that satisfactory designs can be obtained using conventional design approaches even for low data rates, where approximate discretization techniques are so seriously in error as to be invalid. Herein lies the main contribution of the paper: the recognition that the w' domain models the sampling and data-hold operations exactly, regardless of the sampling rate employed, and that the w' variable is analogous to the s variable in the sense that all familiar frequency domain design concepts, procedures, and interpretations can be carried over directly.

Relationships Among z, w, and w'

In the analysis of linear sampled-data systems, use of $z=\exp(sT)$ results in transfer functions that are rational polynomial functions of z. This is in distinction to the corresponding transfer functions in s-domain terms which are transcendental functions of s. It is also the case that the left half of the s plane is mapped into the interior of a unit circle in the z plane. A drawback of the z domain is that conventional design criteria, such as root locus and Bode plots, are more difficult to interpret. Moreover, at high sampling rates, the z plane poles and zeros tend to cluster on the unit circle, creating numerical problems of a substantial magnitude. The region of the z plane corresponding to stable system behavior is interior to the unit circle which prevents the direct application of Routh's stability criteria. Historically (e.g., see Tou[7]), this fact prompted the application of an additional bilinear transformation that maps a function of z into a domain where the region of stability is once again the left half-plane. This is the so-called w transformation, defined by the equation

$$w \triangleq (z-1)/(z+1) \tag{1}$$

One may use root locus and Bode plot methods in the w domain with more facility and insight than would be possible in the z domain, even though each domain contains exactly the same information. The relationship between angular frequency ω and the imaginary part of w, v, is

$$v=\tan\omega T/2 \qquad (v \doteq \omega T/2 \quad \text{for} \quad |\omega| < \pi/2T) \tag{2}$$

However, the w domain still lacks other desirable properties. Most important of these is the property that w approach s as the sampling interval approaches zero. This property is not provided, since

$$w=\frac{z-1}{z+1}=\frac{e^{sT}-1}{e^{sT}+1}=\frac{sT+(sT)^2/2!+\cdots}{2+sT+(sT)^2/2!+\cdots} \tag{3}$$

and in the limit, as $T\to 0$, w approaches zero rather than s. A simple scaling of the w plane changes this situation dramatically. Define

$$w' \triangleq \frac{2}{T}w=\frac{2}{T}\frac{z-1}{z+1}; \qquad z=\frac{1+(T/2)w'}{1-(T/2)w'} \tag{4}$$

as the so-called "w-prime" transformation, wherein

$$w'=\frac{2}{T}\frac{z-1}{z+1}=\frac{2}{T}\frac{e^{sT}-1}{e^{sT}+1}=\frac{2}{T}\frac{sT+(sT)^2/2!+\cdots}{2+sT+(sT)^2/2!+\cdots} \tag{5}$$

In the limit as $T\to 0$ in Eq. (5), w' approaches s.

This property is significant in that it establishes the conceptual basis for defining a quantity in the w' domain which is analogous to frequency in the s domain. Furthermore, the analogy becomes an identity in the limiting case.

We are unable to cite a readily available reference for the transformation given in Eq. (4), even though the relationship is well known to many practicing control engineers (e.g., Stapleford[8] and Franklin and Powell[9]).

One may, of course, use root locus and Bode plot methods in the w' domain as well. However, the relationship between angular frequency ω and the imaginary part of w', v, is

$$v=(2/T)\tan\omega T/2 \qquad (v \doteq \omega \quad \text{for} \quad |\omega| < \pi/2T) \tag{6}$$

The approximate relationship between v and ω is significant in that the designer/analyst may regard v as angular frequency (for $|v|<2/T$) during qualitative phases of design development. The continual conversion to angular frequency units required in the w domain is avoided. Moreover, $(w')^{-1}$ itself is the trapezoidal integration operator analogously to s^{-1} for continuous systems. This is in distinction to the w domain, wherein the trapezoidal integration operator is $(2w/T)^{-1}$. Finally, the unit delay z^{-1}, when expressed in the w' domain, has break parameters that are a function of sampling period T and has the form of a first-order Pade approximant for a transport delay in the s domain:

$$z^{-1}=-\frac{w'-2/T}{w'+2/T} \tag{7}$$

To illustrate another basic relationship that exists between the s domain and the w' domain, consider the z transform for a continuous low-pass filter section

$$H(s)=a/(s+a) \tag{8}$$

obtained assuming that the input signal to the filter has been reconstructed using a zero-order hold (ZOH). The result commonly is called the "pulsed transfer function":

$$H(z)=\left[\frac{1-e^{-sT}}{s}\frac{a}{s+a}\right]^T=\frac{1-e^{-aT}}{z-e^{-aT}} \tag{9}$$

The T superscript is used in Eq. (9) and throughout the paper to indicate that the time function corresponding to the inverse Laplace transform of the bracketed term is to be sampled at a rate of $1/T$ samples/s and then z-transformed. Applying Eq. (4) to Eq. (9) gives

$$H(w')=\frac{-(T/2)w'+1}{\frac{T}{2}\frac{1+e^{-aT}}{1-e^{-aT}}w'+1}=\frac{2}{T}\frac{1-e^{-aT}}{1+e^{-aT}}\frac{-(T/2)w'+1}{w'+\frac{2}{T}\frac{1-e^{-aT}}{1+e^{-aT}}} \tag{10}$$

The equal-order over equal-order nature of Eq. (10) is, of course, a direct consequence of the use of Eq. (4). At first one may feel that the analogy between the s and w' domains is weak, since a proper rational function of s will always map into a rational equal-order over equal-order function of w'. However, this is not the case if zeros at infinity in the s domain are considered, for then the s-domain zeros at infinity correspond to the "extra" finite zeros in the w' plane. For example, Eq. (8) shows that $H(s)$ has a pole at $s=-a$ and a zero at infinity. In the w' plane, the pole at $s=-a$ is mapped into

$$w'=-\frac{2}{T}\frac{1-e^{-aT}}{1+e^{-aT}} \qquad (w' \doteq -a \quad \text{for} \quad |a| < \pi/2T) \tag{11}$$

whereas the zero at $s=\infty$ is mapped into a zero at $w'=2/T$. Obviously, as $T\to 0$, $w'\to s$, the w'-domain pole goes to $-a$ and the w'-domain zero approaches infinity, its proper s-plane location. This is a general result; every pole and zero in the w' plane has its counterpart in the s plane, as long as the zeros at infinity in the s plane are counted. Notice now the

clear resemblance of Eq. (10) to its s-domain counterpart. This is in distinction to the z-domain counterpart, Eq. (9), which has a pole that approaches the unit circle as $T \to 0$.

The zero at $w' = 2/T$ is especially significant. This zero is introduced by the ZOH used to reconstruct the input to $H(s)$. It provides a nonminimum phase contribution, which is the effect of the data-hold sampling rate parameter. This provides another major advantage of the w' domain in comparison to the z domain, since the effect of the data hold and sample rate will be quite apparent in root locus or Bode plots. To emphasize this point, let the input to the continuous filter be reconstructed with another type of data hold called the "slewer data hold." (The slewer data hold results in constant rate output between sampling instants and has no discontinuity at the sampling instants.) Using the slewer, one computes

$$H(z) = \left[\frac{(1-e^{-sT})^2}{Ts^2}\,\frac{a}{s+a}\right]^T \tag{12}$$

$$H(z) = \frac{\left[\left(T-\frac{1}{a}\right)+\frac{e^{-aT}}{a}\right]z+\left[\frac{1}{a}-\left(T+\frac{1}{a}\right)e^{-aT}\right]}{Tz(z-e^{-aT})} \tag{13}$$

or, using Eq. (4),

$$H(w') = \frac{\left[\frac{(T-2/a)+(T+2/a)e^{-aT}}{2(1-e^{-aT})}w'+1\right]\left[-\frac{T}{2}w'+1\right]}{\left[\frac{T}{2}\frac{1+e^{-aT}}{1-e^{-aT}}w'+1\right]\left[\frac{T}{2}w'+1\right]} \tag{14}$$

Observe that the slewer data hold has introduced both a pole and zero in the w'-plane model. Thus it is seen that the use of a zero-order hold introduces a nonminimum phase zero at

Table 1 Representative s- and z-domain transfer functions[a]

$H(s)$	$H(z)$
$\frac{a}{s+a}$	$\frac{1-e^{-aT}}{z-e^{-aT}}$
$\frac{a^2+b^2}{(s+a)^2+b^2}$	$\frac{\left[1-e^{-aT}\left(\cos bT+\frac{a}{b}\sin bT\right)\right]z+\left[e^{-2aT}+\left(\frac{a}{b}\sin bT-\cos bT\right)e^{-aT}\right]}{z^2-2e^{-aT}\cos bTz+e^{-2aT}}$
$\frac{s(a^2+b^2)}{(s+a)^2+b^2}$	$\frac{\left(\frac{a^2+b^2}{b}\right)\left(e^{-aT}\sin bT\right)(z-1)}{z^2-2e^{-aT}\cos bTz+e^{-2aT}}$

[a] Note: input signal is through a zero-order hold.

Table 2 Representative s- and w'-domain transfer functions[a]

$H(s)$	$H(w')$
$\frac{a}{s+a}$	$\frac{1-(T/2)w'}{\frac{T}{2}\frac{1+e^{-aT}}{1-e^{-aT}}w'+1}$
$\frac{a^2+b^2}{(s+a)^2+b^2}$	$\frac{\frac{1+e^{-2aT}-2e^{-aT}\cos bT}{\left(\frac{T^2}{4}\right)[1+2e^{-aT}\cos bT+e^{-2aT}]}\left[\frac{w'}{\frac{1+e^{-2aT}-2e^{-aT}\cos bT}{(T/2)[1-e^{-2aT}-2(a/b)\sin bTe^{-aT}]}}+1\right]\left[\frac{w'}{-2/T}+1\right]}{w'^2+\frac{T(1-e^{-2aT})}{(T^2/4)[1+2e^{-aT}\cos bT+e^{-2aT}]}w'+\frac{1-2e^{-aT}\cos bT+e^{-2aT}}{(T^2/4)[1+2e^{-aT}\cos bT+e^{-2aT}]}}$
$\frac{s(a^2+b^2)}{(s+a)^2+b^2}$	$\frac{\left(\frac{T\frac{a^2+b^2}{b}e^{-aT}\sin bT}{(T^2/4[1+2e^{-aT}\cos bT+e^{-2aT}]}\right)w'\left(\frac{w}{-(2/T)}+1\right)}{w'^2+\frac{T(1-e^{-2aT})}{(T^2/4)[1+2e^{-aT}\cos bT+e^{-2aT}]}w'+\frac{1-2e^{-aT}\cos bT+e^{-2aT}}{(T^2/4)[1+2e^{-aT}\cos bT+e^{-2aT}]}}$

[a] Note: input signal is through a zero-order hold.

$w' = 2/T$ [refer to Eq. (10)], whereas the slewer introduces *both* a pole and zero. Finally, note that Eq. (14) reduces to

$$\lim_{T\to 0} H(w') = a/(w'+a) \tag{15}$$

as was the case with the zero-order hold.

Tables 1 and 2 summarize the relationships between the various domains for three different filter sections assuming the use of a zero-order hold. Example corresponding transfer functions, using T as a parameter, in the s and w' domains are given in Table 3. These enable one to obtain a feel for the relative positioning of poles and zeros.

Thus far, three important properties of the w' domain have been enumerated: 1) $w' \to s$ as $T \to 0$; 2) the nonminimum phase effects of the data holds become clearly evident; and 3) conventional methods for stability analyses continue to be applicable, since the left half of the w' plane corresponds to the left half of the s plane.

A most important property of the w' domain which remains to be shown is as follows: conventional frequency domain synthesis methods (both scalar and vector) continue to be applicable, even when the sampling rate is so low as to cause large differences between s-plane and w'-plane pole and zero locations for a given plant. This property is the topic of the next two sections.

Illustrative Design Problems

Short-Period Aircraft Model

Conventional frequency domain design methods are directly applicable in the w' domain. This will be demonstrated in two stages. In this section, we first consider the design of a stability augmentation system using a representative model of a short-period aircraft. (The technical details of the models used in this section and the next have been discussed by Whitbeck.[10]) The use of the second-order model will allow us to illustrate clearly the manner in which the nonminimum phase contribution of the data hold affects closed-loop system properties and responses. (Furthermore, these effects are different for a disturbance input from what they are for a command input.) The short-period model will, however, tend to have modal frequencies well below the folding frequency, even for data rates as low as 10 samples/s. Thus, the most dramatic effect that folding (or aliasing) may have upon the plant w' transfer functions will not be evident. Therefore, in the next section we consider a fourth-order aircraft model that includes a high-frequency, lightly damped bending mode for which the effects of folding are dramatic. This will enable us to demonstrate that the w' domain continues to yield satisfactory closed-loop designs even when the differences between the s-domain and w'-domain modal representations are large.

Table 3 Example second-order s- and w'-domain transfer functions[a]

$H(s)$	$H(w')$
$\dfrac{5}{s^2+2s+5}$	$\dfrac{5.025028\left(\dfrac{w'}{599.4003477}+1\right)\left(-\dfrac{w'}{20}+1\right)}{w'^2+2.018401616w'+5.025028}$ $T=0.1$
$\dfrac{5s}{s^2+2s+5}$	$\dfrac{5.004086913[-(w'/20)+1]w'}{w'^2+2.018401616w'+5.025028}$ $T=0.1$

[a] Note: Input signal is through a zero-order hold.

Consider first the simplified aircraft model of Eq. (16):

$$\begin{bmatrix} \dot{q} \\ \dot{\alpha} \end{bmatrix} = \begin{bmatrix} -1 & -37 \\ 1 & -3 \end{bmatrix} \begin{bmatrix} q \\ \alpha \end{bmatrix} + \begin{bmatrix} -50 \\ 0 \end{bmatrix} \delta_e + \begin{bmatrix} -37 \\ -3 \end{bmatrix} \alpha_g \tag{16}$$

Suppose that the continuous controller is designed using the multiloop analysis technique of McRuer et al.[11] The block diagram of Fig. 1 defines the closed-loop configuration with postulated compensation networks H_1, H_2, and H_3. In Fig. 1, H_1, H_2, and H_3 are to be determined (designed), R is the command input, and x_1 and x_2 are used to represent the states q and α, respectively. Application of the multiloop analysis method yields the matrix of closed-loop transfer functions directly. The theoretical details of the multiloop analysis method are documented in Chap. 3 of Ref. 11:

$$\begin{bmatrix} x_1 \\ \hline x_2 \end{bmatrix} = \frac{\left[\begin{array}{c|c} N^{x_1}_{\delta_e} H_3 & N^{x_1}_{\alpha_g} + H_2 H_3 N^{x_1 x_2}_{\alpha_g \delta_e} \\ \hline N^{x_2}_{\delta_e} H_3 & N^{x_2}_{\alpha_g} + H_1 H_3 N^{x_2 x_1}_{\alpha_g \delta_e} \end{array}\right] \left[\begin{array}{c} R \\ \hline \alpha_g \end{array}\right]}{\Delta + H_2 H_3 N^{x_2}_{\delta_e} + H_1 H_3 N^{x_1}_{\delta_e}} \tag{17}$$

The various numerators of Eq. (17) are found using Cramer's rule applied to the Laplace transform of Eq. (16) [see Eq. (18)]:

$$\begin{bmatrix} s+1 & 37 \\ -1 & s+3 \end{bmatrix} \begin{bmatrix} x_1 \\ x_2 \end{bmatrix} = \begin{bmatrix} -50 & -37 \\ 0 & -3 \end{bmatrix} \begin{bmatrix} \delta_e \\ \alpha_g \end{bmatrix} \tag{18}$$

$N^{x_2}_{\delta_e}$, for example, is found by substituting the δ_e column on the right-hand side of Eq. (18) into the x_2 column on the left-hand side of Eq. (18) and evaluating the determinant of the array that results. Δ is the characteristic open-loop polynomial and is the determinant of the left-hand matrix in Eq. (18). To illustrate,

$$\Delta = \begin{vmatrix} s+1 & 37 \\ -1 & s+3 \end{vmatrix} = s^2+4s+40 = (s+2)^2+(6)^2 \tag{19}$$

$$N^{x_2}_{\delta_e} = \begin{vmatrix} s+1 & -50 \\ -1 & 0 \end{vmatrix} = -50 \tag{20}$$

$$N^{x_1}_{\delta_e} = -50(s+3) \tag{21}$$

$$N^{x_1}_{\alpha_g} = -37s \tag{22}$$

$$N^{x_2}_{\alpha_g} = -(3s+40) \tag{23}$$

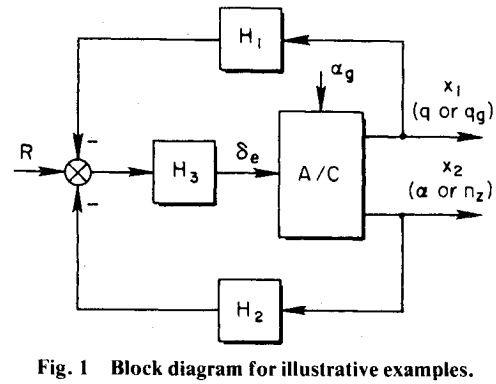

Fig. 1 Block diagram for illustrative examples.

The numerators of the "second kind" (coupling numerators), $N^{x_1 x_2}_{\alpha_g \delta_e} = -N^{x_1 x_2}_{\alpha_g \delta_e}$, are found by making *two* column substitutions and computing the determinant of the resulting array:

$$N^{x_2 x_1}_{\alpha_g \delta_e} = \begin{vmatrix} -50 & -37 \\ 0 & -3 \end{vmatrix} = 150 = -N^{x_1 x_2}_{\alpha_g \delta_e} \tag{24}$$

Substitution of this equation into Eq. (17) gives

$$\begin{bmatrix} x_1 \\ \hline x_2 \end{bmatrix} = \frac{\left[\begin{array}{c|c} -3.75[(s/3)+1]H_3 & -0.925s - 3.75H_2H_3 \\ \hline -1.25H_3 & -1[(s/13.33)+1] + 3.75H_1H_3 \end{array}\right] \begin{bmatrix} R \\ \hline \alpha_g \end{bmatrix}}{\left(\frac{s^2}{40} + \frac{4}{40}s + 1\right) - 1.25H_2H_3 - 3.75\left(\frac{s}{3} + 1\right)H_1H_3} \tag{25}$$

From this point on, the design effort for a continuous controller would focus on the specification of H_1, H_2, and H_3 in order to achieve desirable closed-loop characteristics. Bode plots, Nyquist diagrams, root loci, etc., could be used to achieve this goal. Rather than dwell on these well-understood facets of the frequency domain synthesis, we turn our attention instead to the synthesis of a (single-rate) digital controller for the plant described by Eq. (16).

Suppose that Fig. 1 is modified to explicitly account for A/D and D/A conversions. A simplified representation of the digital control system is shown in Fig. 2, where the elements interior to the dashed box represent the continuous elements (plant and data hold) of the overall system. The input R is assumed to undergo an A/D conversion that is modeled adequately by a sampler. All of the remaining elements of Fig. 2 are to be implemented on a digital computer. For simplicity of presentation, the data hold is assumed to be a zero-order hold; however, the synthesis procedure that we are about to explore will be directly applicable for other types of data holds as well.

Taking the z transform of the first-order set of differential equations given in Eq. (16) gives:

$$\left[\begin{array}{c|c} z - 0.752776009 & 2.850789304 \\ \hline -0.07704836 & z - 0.59867929 \end{array}\right] \begin{bmatrix} x_1(z) \\ \hline x_2(z) \end{bmatrix} = \left[\begin{array}{c|c} -4.490576597 & -2.850789304 \\ \hline -0.212719539 & -0.401320710 \end{array}\right] \begin{bmatrix} \delta_e \\ \hline \alpha_g \end{bmatrix} \tag{26}$$

Equation (26) may be developed from Eq. (16) using either time domain or frequency domain approaches. We have assumed that the gust input is sampled at $1/T$ samples/s and held. This is somewhat at variance with the physical reality of the problem, since the plant is actually excited by a continuous disturbance. This assumption has been made merely because it has a simplifying effect upon this illustrative problem. It is not essential.

Because of the sampling assumption on α_g, one can proceed conceptually in terms of a completely discretized system; the state vector has been sampled and fed to the digital computer, as has the scalar input R. One may think of Fig. 1 and Eq. (17) in terms of the z or w' domain, as well as in terms of the s domain. That is, in Eq. (17) consider $x_1(s)$ to be replaced by $x_1(z)$, $N^{x_2}_{\delta_e}(s)$ by $N^{x_2}_{\delta_e}(z)$, etc. Thus, one can proceed to generate the z domain equivalent of Eq. (25), given a sampling rate (assume 10 samples/s), and upon making computations of the characteristic polynomial and numerators of the first and second kinds:

z Domain

$$\begin{bmatrix} x_1 \\ \hline x_2 \end{bmatrix} = \frac{\left[\begin{array}{c|c} (-4.491z + 3.295)H_3 & (-2.851z + 2.851) + H_2H_3(-1.196) \\ \hline (-0.2127z - 0.1859)H_3 & (-0.4013z + 0.0825) + H_1H_3(1.196) \end{array}\right] \begin{bmatrix} R(z) \\ \hline \alpha_g(z) \end{bmatrix}}{(z^2 - 1.352z + 0.6703) + H_2H_3(-0.2127z - 0.1859) + H_1H_3(-4.491z + 3.295)} \tag{27}$$

The closed-loop z-domain equation is not interpreted easily by methods useful for interpreting the closed-loop s-domain equations. To facilitate interpretation, it is our assertion that the w' transform should be applied to Eq. (27); i.e., $z = [1 + (T/2)w']/[1 - (T/2)w']$. The result is given in Eq. (28). The reader should compare the numerical values for the gains and break frequencies in Eq. (28) with the corresponding quantities in Eq. (25). Close correspondence for many of these numerical values should be noted:

w' Domain

$$\begin{bmatrix} x_1 \\ \hline x_2 \end{bmatrix} = \frac{\left[\begin{array}{c|c} -3.750000159\left(\frac{w'}{3.072} + 1\right)H_3\left(1 - \frac{w'}{20}\right) & -0.89404w'\left(1 - \frac{w'}{20}\right) - 3.75H_2H_3\left(1 - \frac{w'}{20}\right)^2 \\ \hline -1.250000067\left(\frac{w'}{296.81} + 1\right)H_3\left(1 - \frac{w'}{20}\right) & -1.000000051\left(\frac{w'}{13.1823}\right) + 3.75H_1H_3\left(1 - \frac{w'}{20}\right)^2 \end{array}\right] \begin{bmatrix} R \\ \hline \alpha_g \end{bmatrix}}{\left(\frac{w'^2}{42.2089} + \frac{4.3641}{42.2089}w' + 1\right) - 1.250000067\left(\frac{w'}{296.81} + 1\right)H_2H_3\left(1 - \frac{w'}{20}\right) - 3.750000159\left(\frac{w'}{3.0718} + 1\right)H_1H_3\left(1 - \frac{w'}{20}\right)} \tag{28}$$

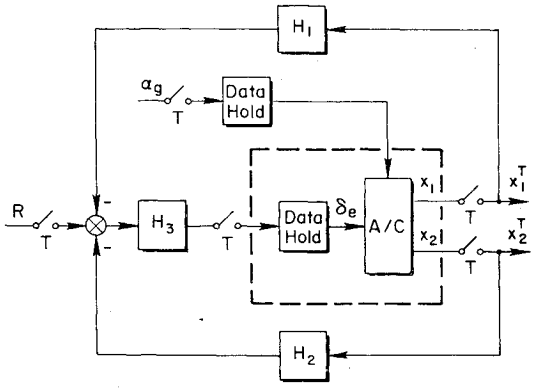

Fig. 2 Digital control block diagram.

It is our contention that the effects of the sample/hold operation, the data rate, etc., are readily apparent in Eq. (28). Comparing Eqs. (28) and (25), we find the following:

1) Numerators of the first kind pick up additional zeros at $2/T$ in such a way that they have the same degree as the characteristic polynomial.

2) Numerators of the second kind pick up additional zeros at $2/T$ in such a way that they are equal in degree to the characteristic polynomial.

3) Every entry in the s-domain equation can be considered to be equal-order over equal-order if the zeros at infinity are included.

4) Every entry in the w'-plane equation is equal-order over equal-order. Zeros at infinity in the s plane move to either $2/T$ or some other location, for example,

$$-1.25H_3(s) \rightarrow -1.25\left(\frac{w'}{297}+1\right)\left(1-\frac{w'}{20}\right)H_3(w') \qquad (29)$$

5) The numerical values of gains and time constants in the w' plane are very similar to their s-plane counterparts. (Although not demonstrated in this example, this observation holds only for modes having an s-plane modal frequency that is well below the folding frequency. The fact that this observation holds true only under the stated conditions does not limit validity of the w'-plane analysis techniques in any way when the stated conditions are not satisfied. That this is so is demonstrated in the next section.)

Thus, one may proceed in the w' domain using all of the familiar synthesis tools of the s domain. The direct digital design in the w' domain, however, proceeds with additional explicit knowledge of the nonminimum phase effects introduced by the A/D and D/A conversion through the zeros introduced at $2/T$ (equal to 20 rad/s for this example). If these nonminimum phase effects become significant (the zeros move closer to the origin as the sampling rate is decreased), then they can be regarded in exactly the same manner and treated using the same techniques as are used in the s domain.

The actual synthesis will not be carried out, since the prime objective was to highlight the analogy between the closed-loop transfer functions in the s, z, and w' domains. A synthesis will be carried to completion for the more complex aircraft model used in the next section.

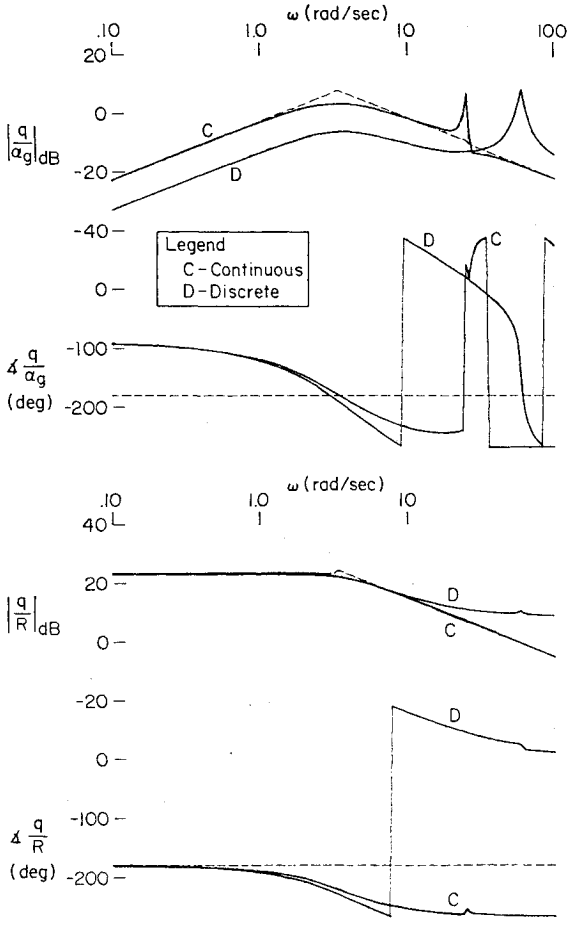

Fig. 3 Bode plots q/α_g, q/R.

Short-Period Aircraft with Bending Mode

It remains to demonstrate the utility of the w' domain in the face of substantial folding effects. This can be done by modifying the example of the previous section to present a more realistic design situation. Specifically, the aircraft model is modified to include a lightly damped bending mode at 25 rad/s (this will be close to the 10 samples/s aliasing frequency of 31.2 rad/s) and to include accelerometer and rate gyro output equations. Thus, we shall have one control input, one disturbance input, four components in the state vector, and two components in the output vector. The details of the model are given by Whitbeck.[10] For our present purposes, it is sufficient to modify our interpretation of the block diagram of Fig. 1. Let n_z be x_1, and q_g be x_2. The open-loop transfer functions are given in Eqs. (30) and (31):

s Domain

$$\begin{bmatrix} x_1 \\ x_2 \end{bmatrix} = \begin{bmatrix} n_z \\ q_g \end{bmatrix} = \frac{\begin{bmatrix} -117.72[0.141, 35.2][-0.0314, 26.357] \\ -3.7975\left[\frac{s}{3.1045}+1\right][0.0152, 24.346] \end{bmatrix}}{[0.355, 6.675][0.01, 25]}\,\delta_e \qquad (30)$$

w' Domain ($T=0.1$)

$$\begin{bmatrix} x_1 \\ x_2 \end{bmatrix} = \begin{bmatrix} n_z \\ q_g \end{bmatrix} = \frac{\begin{bmatrix} -123.5\left(-\frac{w'}{27.53}+1\right)\left(\frac{w'}{13020}+1\right)[0.1, 32.62] \\ -3.7974\left(\frac{w'}{3.22}+1\right)\left(-\frac{w'}{20}+1\right)[0.069, 107.22] \end{bmatrix}}{[0.3789, 6.864][0.0417, 60.137]}\,\delta_e \qquad (31)$$

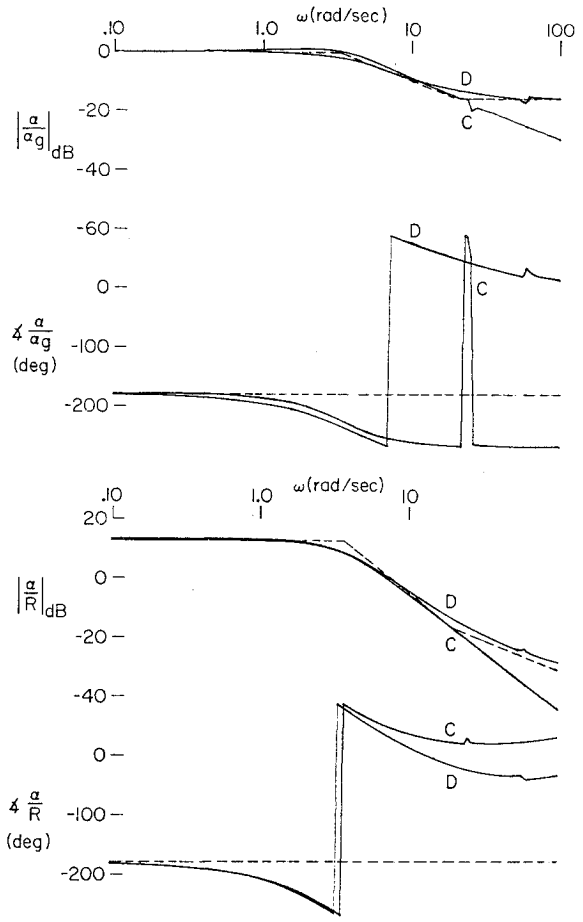

Fig. 4 Bode plots α/α_g, α/R.

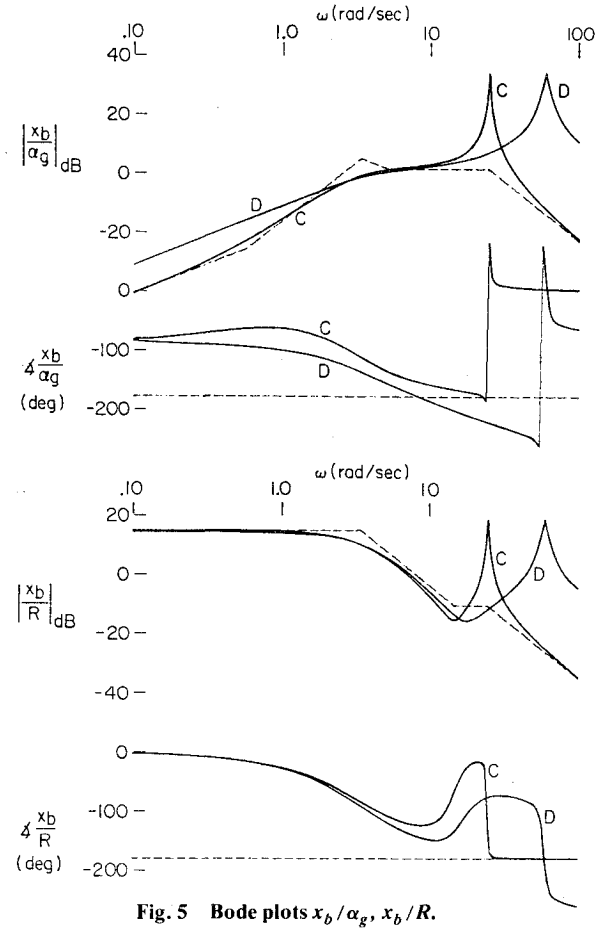

Fig. 5 Bode plots x_b/α_g, x_b/R.

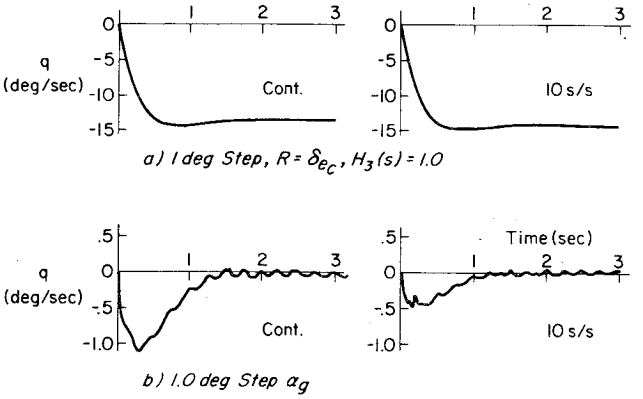

Fig. 6 q transient responses of continuous and digitally controlled systems.

In these equations, quadratic factors $[s^2+2\zeta\omega_n s+\omega_n^2]$ have been shown in the shorthand form $[\zeta, \omega_n]$. Comparison of the corresponding numerator and characteristic polynomial roots in Eqs. (30) and (31) leads to the following observations:

1) The short-period quadratic is essentially the same in either the s or w' domain.

2) The bending mode at the 25-rad/s in the s domain has been shifted upward to 60/s in the w' domain. (A still lower sampling rate could shift it downward.)

3) The n_z numerator, which is equal-order over equal-order in the s domain, does not have the zero at $w'=2/T$.

Clearly, we now have a design problem where the folding effects are significant. However, the closed-loop design still can be synthesized using conventional multiloop frequency domain techniques. The following compensation was arrived at using mainly root locus techniques:

$$H_1H_3 = 0.006 \tag{32}$$

$$H_2H_3 = 0.0085\frac{w'+1.644}{w'+3.273} \tag{33}$$

This translates back into the z domain (and gives the required recursion equation for the discrete control law) as

$$H_1H_3 = 0.006 \tag{34}$$

$$H_2H_3 = \frac{0.0079z-0.0067}{z-0.71875} \tag{35}$$

The closed-loop relationships are given by Eq. (17), which is valid for both the s and w' domains. Rather than give numerical comparison between s and w' using Eq. (4), as was done in the previous section, it is our preference to show Bode plots for the closed-loop system in the s and w' domains. The Bode plots for the transfer functions of interest are plotted in Figs. 3-5. Notice in particular the effect of the nonminimum phase zero on the magnitude and phase plots.

At this point, we come face to face with the central question: "Are s-domain design procedures and concepts effective in the w' domain?" We proceeded with the design in the w' domain on the hypothesis that these design procedures and concepts are effective and with the knowledge that the w'-domain transfer functions for the plant properly and comprehensively incorporate all of the effects of the data hold and sampling rate for all modes. To demonstrate that this hypothesis is correct, we must check the time responses for the discretely controlled system to see if they are acceptable. This is done for the q variable in Fig. 6. Notice that there is no basis to conclude that the performance of the digitally controlled system is inferior to that of the continuously controlled one, or vice versa. In fact, the use of an accelerometer

feedback gain of 0.006 has resulted in a lower q/α_g amplitude ratio at lower frequencies for the digitally controlled system.

Conclusions

Analogies between system formulations in the s and w' domains have been drawn. To arrive at the w'-plane formulation, one first must discretize the problem by means of a valid mathematical technique if the effects of data holds are to be represented exactly. This leads to a statement of the discretized problem in the z domain. The z-domain statement of the problem then is converted to a w'-domain statement by means of a bilinear algebraic transformation.

It has been demonstrated that direct digital control law synthesis in the w' domain is a viable and practical alternative to design by emulation of a continuous system. Key properties of the w' domain have been stated, and the "visibility" of data-hold and sampling rate nonminimum phase effects in the w' domain has been demonstrated. More important is the fact that conventional frequency domain design procedures, such as multiloop analysis, Bode plots, root locus, etc., are valid and useful procedures in the w' domain even in the presence of significant aliasing. Finally, there is the convenience resulting from the fact that the imaginary part of w', ν, approximates angular frequency ω for $|\omega| < \pi/2T$ or $|\nu| < 2/T$. The impact of this is that the control designer now can synthesize digital controllers using considerably lower sampling rates than are required when an emulation design approach is used. Furthermore, the direct digital control law synthesis approach presented here requires no new analytical techniques beyond those classical frequency domain procedures required by the emulation design approach. The analytical techniques are merely applied and interpreted in the novel manner that we have described in this paper.

Acknowledgment

This work was performed for the Air Force Flight Dynamics Laboratory (AFFDL/FGC), Wright-Patterson Air Force Base, Ohio, under Contract F33615-77-C-3026.

References

[1] Fryer, W.D. and Schultz, W.C., "A Survey of Methods for Digital Simulation of Control Systems," Cornell Aeronautical Lab., Buffalo, N.Y., XA-1681-E-1, July 1964.

[2] Madwed, A., "Number Series Method of Solving Linear and Nonlinear Differential Equations," Massachusetts Inst. of Technology, Instrumentation Lab., Cambridge, Mass., 6445-T-26, April 1950.

[3] Tustin, A., "A Method of Analyzing the Behavior of Linear Systems in Terms of Time Series," *Proceedings of the IEE,* Vol. 94, Pt. IIA, Jan. 1947, pp. 130-142.

[4] Borow, M.S., Gaabo, R.O., Hendrick, R.C. et al., "Navy Digital Flight Control Development," Honeywell, Inc., 21857-FR, Dec. 1972.

[5] "Tactical Aircraft Guidance System Development Program Flight Test Phase Report," Army Air Mobility Research and Development Lab., USAAMRDL-TR-73-89A and -89B, April 1974.

[6] Bailey, D.G. and Folkesson, K., "Software Control Procedures for the SAAB JA-37 Digital Automatic Flight Control System," *Proceedings of the AIAA Guidance and Control Conference,* AIAA, New York, Aug. 1976, pp. 122-129.

[7] Tou, J.T., *Digital and Sampled Data Control Systems,* McGraw-Hill, New York, 1959, pp. 244-249, 465-268.

[8] Stapleford, R.L., "Digital Flight Control Design Procedures," Systems Technology, Inc., Hawthorne, Calif., Memo., Aug. 20, 1974.

[9] Franklin, G.F. and Powell, J.D., "Digital Control, Notes Prepared for E207," Stanford Univ., Jan. 1976, pp. 5.19-5.22.

[10] Whitbeck, R.F., "Feasibility of a Low Rate Digital Controller for the A-7," Systems Technology, Inc., Hawthorne, Calif., TR-503-1, Aug. 1976.

[11] McRuer, D.T., Ashkenas, I.L., and Graham, D., *Aircraft Dynamics and Automatic Control,* Princeton Univ. Press, Princeton, N.J., 1973.